Challenges in Panchromatic Modelling with
Next Generation Facilities
Proceedings IAU Symposium No. 341, 2018
M. Boquien, E. Lusso, C. Gruppioni & P. Tissera, eds.

doi:10.1017/S1743921319002618

Census of Lyα, [OIII]5007, Hα, and [CII]158μm line emission with ∼1000 galaxies at $z = 4.9 - 7.0$ revealed with Subaru/HSC, Spitzer, and ALMA

Yuichi Harikane

Institute for Cosmic Ray Research, The University of Tokyo, 5-1-5 Kashiwanoha, Kashiwa, Chiba 277-8582, Japan

Department of Physics, Graduate School of Science, The University of Tokyo, 7-3-1 Hongo, Bunkyo, Tokyo, 113-0033, Japan
email: hari@icrr.u-tokyo.ac.jp

Abstract. We investigate rest-frame UV to far-infrared emission lines and SEDs from 1124 galaxies at $z = 4.9-7.0$. Our sample is composed of 1092 Lyα emitters (LAEs) at $z = 4.9-7.0$ identified by Subaru/Hyper Suprime-Cam (HSC) narrowband surveys and 34 galaxies at $z = 5.148-7.508$ with deep [CII]158μm ALMA data. The SEDs clearly show flux excesses in the Spitzer/IRAC 3.6 and 4.5μm bands, suggesting strong rest-frame optical emission lines of [OIII] and/or Hα. We model the galaxy SEDs with a flexible code combining stellar population and photo-ionization models (BEAGLE; Chevallard & Charlot 2016), and investigate relations between the emission lines of Lyα, [OIII], Hα, and [CII]. We find 1) a positive correlation between the rest-frame Hα equivalent width (EW) and the Lyα EW, $EW^0_{\mathrm{Ly}\alpha}$, 2) an interesting turn-over trend that the [OIII]/Hα flux ratio increases in $EW^0_{\mathrm{Ly}\alpha} \simeq 0-30$ Å, and then decreases out to $EW^0_{\mathrm{Ly}\alpha} \simeq 130$ Å, and 3) a $> 99\%$ anti-correlation between a [CII] luminosity to star-formation rate ratio $L_{[\mathrm{CII}]}/SFR$) and $EW^0_{\mathrm{Ly}\alpha}$. Modeling with BEAGLE also suggests that a simple anti-correlation between $EW^0_{\mathrm{Ly}\alpha}$ and metallicity explains self-consistently all of the relations of Lyα, Hα, [OIII]/Hα, and [CII] in our study, indicative of detections of very metal-poor ($\sim 0.03 Z_\odot$) galaxies with $EW^0_{\mathrm{Ly}\alpha} \sim 200$ Å.

Keywords. galaxy evolution, galaxy formation, high-redshift galaxy

1. Introduction

Probing physical conditions of the inter-stellar medium (ISM) is fundamental in understanding star formation and gas reprocessing in galaxies across cosmic time. Early ALMA observations found surprisingly weak [CII]158μm emission in Lyα emitters (LAEs) at $z \sim 6-7$ ([CII] deficit; e.g., Ouchi *et al.* 2013; Schaerer *et al.* 2015; Maiolino *et al.* 2015). A theoretical study discusses that the [CII] deficit can be explained by very low metallicity (0.05 $Z_\odot$) in the ISM (Vallini *et al.* 2015; Olsen *et al.* 2017). Thus estimating metallicities of the high-redshift galaxies is crucial to our understanding of the origin of the [CII] deficit.

The ISM property is also important for cosmic reionization. Observations by the Planck satellite and high redshift UV luminosity functions (LFs) suggest that faint and abundant star-forming galaxies dominate the reionization process (e.g., Robertson *et al.* 2015), and understanding ionizing properties of such star forming galaxies is important. Various studies constrain ionizing photon production efficiencies of star forming galaxies to be $\log\xi_{\mathrm{ion}}/[\mathrm{Hz\ erg}^{-1}] = 24.8-25.3$ at $z \sim 0-2$ (e.g., Matthee *et al.* 2017; Shivaei *et al.*

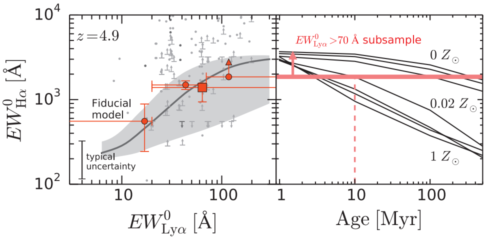

Figure 1. Left panel: Hα EWs as a function of Lyα EWs at $z = 4.9$. The red square and circles are the results from the stacked images of the subsamples, and the gray dots show the EWs of the individual objects detected in the [3.6] and/or [4.5] bands. The upward and downward arrows represent the 2σ lower and upper limits, respectively. The dark gray curve and the shaded region show the prediction from the fiducial model. **Right panel:** Inferred stellar age and metallicity from the constrained $EW^0_{\mathrm{H}\alpha}$. The red solid line shows the lower limit of $EW^0_{\mathrm{H}\alpha} \gtrsim 2000$ Å in the 70 Å $< EW_{\mathrm{Ly}\alpha} <$ 1000 Å subsample at $z = 4.9$. The black curves represent $EW^0_{\mathrm{H}\alpha}$ calculated in Inoue (2011) with metallicities of $Z = 0$, 5×10^{-6}, 5×10^{-4}, 0.02, 0.2, 0.4, and 1 $Z_\odot$.

2017). Since the faint star-forming galaxies are expected to be strong line emitters, it is important to estimate ξ_{ion} of LAEs at higher redshift, as their ISM properties are likely more similar to the ionizing sources.

2. Data & Analysis

We use LAE samples at $z = 4.9$, 5.7, 6.6, and 7.0 selected with the NB filters of $NB718$, $NB816$, $NB921$, and $NB973$, respectively (Shibuya *et al.* 2018; Itoh *et al.* 2018 Zhang *et al.* in prep.), obtained in our Subaru/Hyper Suprime-Cam (HSC) survey (Aihara *et al.* 2018b). We divide our LAE samples into subsamples by the Lyα equivalent width (EW) bins. We cut out 12" × 12" images of the LAEs in HSC $grizyNB718NB816NB921NB973$ ($grizyNB816NB921$), VIRCAM JHK_s (WFCAM JHK), and IRAC [3.6][4.5] bands in the UD-COSMOS (UD-SXDS) field. Then we generate median-stacked images of the subsamples in each band.

We generate the model SEDs at $z = 4.9$, 5.7, 6.6, and 7.0 using BEAGLE (Chevallard & Charlot 2016). We estimate rest-frame optical emission line fluxes by comparing the stacked SEDs with the model SEDs. We calculate the flux differences between the stacked SEDs and the model SEDs in the [3.6] band at $z = 4.9$, and [3.6] and [4.5] bands at $z = 5.7$, 6.6, and 7.0. The flux differences are corrected for dust extinction with the τ_{V} values in the models, assuming the Calzetti *et al.* (2000) extinction curve. We estimate the Hα, Hβ, and [OIII]λ5007 line fluxes from these flux differences.

In addition to our HSC LAE samples, we compile previous ALMA and PdBI observations targeting [CII]158μm in galaxies at $z > 5$. We use results of 34 galaxies from the literature (see Table 3 in Harikane *et al.* 2018).

3. Results

The left panel in Figure 1 shows rest-frame Hα EWs ($EW^0_{\mathrm{H}\alpha}$) as a function of Lyα EWs at $z = 4.9$. The Hα EW increases from ~600 Å to > 1900 Å with increasing Lyα EW. This high $EW^0_{\mathrm{H}\alpha}$ value indicates very young stellar age of < 10 Myr or very low metallicity of < 0.02 $Z_\odot$ (the right panel in Figure 1).

We estimate the ionizing photon production efficiencies of the $z = 4.9$ LAEs from their Hα fluxes and UV luminosities. The left panel in Figure 2 shows estimated ξ_{ion} values as a function of UV magnitude. We calculate the values of the ξ_{ion} in two cases; $f^{\mathrm{ion}}_{\mathrm{esc}} = 0$ and $f^{\mathrm{ion}}_{\mathrm{esc}} = 0.1$. The ionizing photon production efficiency is estimated to be logξ_{ion}/

https://doi.org/10.1017/S1743921319002618 Published online by Cambridge University Press

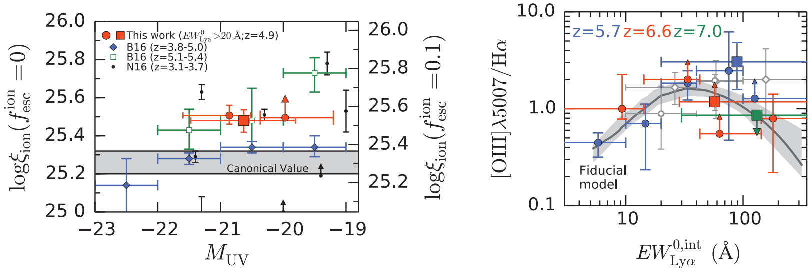

Figure 2. Left panel: Inferred ionizing photon production efficiencies of the LAEs at $z = 4.9$ as a function of UV magnitude. The left and right axes represent the efficiencies with the ionizing photon escape fractions of 0 and 10%, respectively. The red circles and square show the results of the subsamples divided by $EW^0_{Ly\alpha}$, and the upward arrow represents the 2σ lower limit. The ξ_{ion} values of LBGs at $z = 3.8-5.0$ ($z = 5.1-5.4$) in Bouwens *et al.* (2016) are represented as the blue diamonds (green open squares). We plot the ξ_{ion} values of LAEs at $z = 3.1-3.7$ (Nakajima *et al.* 2016) with the black circles. The gray shaded region indicates typically assumed ξ_{ion} (see Table 2 Bouwens *et al.* 2016). **Right panel:** [OIII]/Hα ratio as a function of the Lyα EW. The blue, red, and green circles and squares are the [OIII]λ5007/Hα flux ratios at $z = 5.7$, 6.6, and 7.0, respectively. The open gray diamonds and circles are the ratios of $z = 2.5$ and 0.3 galaxies (Trainor *et al.* 2016; Cowie *et al.* 2011), respectively. We also plot the fitting result of the fiducial model with the dark gray curve with the shaded region representing the 1σ uncertainty.

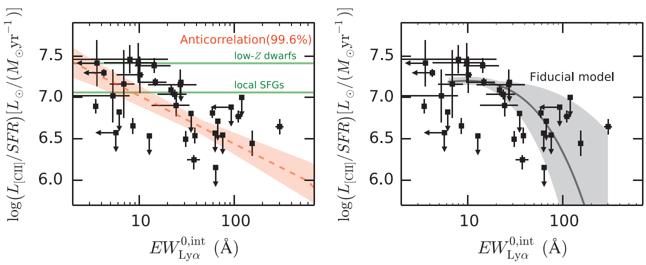

Figure 3. Left panel: Ratio of the [CII] luminosity to the SFR as a function of rest-frame Lyα EW. We find the anti-correlation in the $L_{[CII]}/SFR - EW^{0,int}_{Ly\alpha}$ plane at the 99.6% confidence level. The green horizontal lines show the $L_{[CII]}/SFR$ ratios for low-metallicity dwarf galaxies and local star-forming galaxies in De Looze *et al.* (2014) for $SFR = 10\ M_\odot yr^{-1}$. The red-dashed line and the shaded region denote the best-fit $L_{[CII]}/SFR - EW^{0,int}_{Ly\alpha}$ relation. **Right panel:** Same as the left panel but with the prediction from the fiducial model.

[Hz erg^{-1}] $= 25.48^{+0.06}_{-0.06}$ for the $EW^0_{Ly\alpha} > 20$ Å subsample with $f^{ion}_{esc} = 0$. This value is systematically higher than those of LBGs at the similar redshift and UV magnitude ($\log\xi_{ion}$/[Hz erg^{-1}] $\simeq 25.3$; Bouwens *et al.* 2016) by 60−100%.

The [OIII]/Hα ratios of the $z = 5.7$, 6.6, and 7.0 LAEs are presented in the right panel in Figure 2. We find that the ratio increases with increasing $EW^0_{Ly\alpha}$ from 7 Å to 20 Å, then decreases to ∼130 Å, showing the turn-over trend at the 2.3σ confidence level.

In the left panel in Figure 3, we plot the ratios of the [CII] luminosity to SFR, $L_{[CII]}/SFR$ as a function of Lyα EW corrected for the IGM absorption, $EW^{0,int}_{Ly\alpha}$. We find an anti-correlation in the $L_{[CII]}/SFR - EW^{0,int}_{Ly\alpha}$ plane at the 99.6% confidence level.

4. Discussion

We investigate physical quantities explaining our observed [OIII]/Hα ratios as a function of Lyα EW. We simply parameterize the metallicity, Z_{neb}, the ionization parameter,

$U_{\rm ion}$, and the stellar age with the Lyα EW in units of Å. We fit our observational results of the [OIII]/Hα ratios with this model, and the best-fit relations with 1σ errors are

$$\log Z_{\rm neb} = -0.33^{+0.16}_{-0.11}\left(\log EW^{0,\rm int}_{\rm Ly\alpha}\right)^2 + 0.35^{+0.10}_{-0.18}, \quad (4.1)$$

$$\log U_{\rm ion} = -0.09^{+0.66}_{-0.22}\log EW^{0,\rm int}_{\rm Ly\alpha} - 2.58^{+0.33}_{-0.81}, \quad (4.2)$$

$$\log {\rm Age} = -0.29^{+1.66}_{-0.77}\log EW^{0,\rm int}_{\rm Ly\alpha} + 8.90^{+0.47}_{-3.21}. \quad (4.3)$$

The result suggests an anti-correlation between the metallicity and the Lyα EW, implying the very metal-poor ISM ($\sim$0.03 $Z_\odot$) in the galaxies with $EW^{0,\rm int}_{\rm Ly\alpha} \sim 200$ Å (see also; Nagao *et al.* 2007). Hereafter, we call this model "the fiducial model". We find that this fiducial model agrees well with the observed $EW^0_{\rm H\alpha} - EW^0_{\rm Ly\alpha}$ relation (the left panel in Figure 1). The fiducial model can also nicely explains the $L_{\rm [CII]}/SFR - EW^{0,\rm int}_{\rm Ly\alpha}$ anti-correlation (the right panel in Figure 3), indicating that the [CII] deficit in high Lyα EW galaxies may be due to the low metallicity.

References

Aihara, H., Arimoto, N., Armstrong, R., Arnouts, S., Bahcall, A., Bickerton, S., Bosch, J., Bundy, K., *et al.* 2018b, *PASJ*, 70, S4

Bouwens, R. J., Smit, R., Labbé, I., Franx, M., Caruana, J., Oesch, P., Stefanon, M., & Rasappu, N. 2016, *ApJ*, 831, 176

Calzetti, D., Armus, L., Bohlin, R. C., Kinney, L., Koornneef, J., & Storchi-Bergmann, T. 2000, *ApJ*, 533, 682

Chevallard, J. & Charlot, S. 2016, *MNRAS*, 462, 1415

Cowie, L. L., Barger, A. J., & Hu, E. M. 2011, *ApJ*, 738, 136

De Looze, I., Cormier, D., Lebouteiller, V., Madden, S., Baes, M., Bendo, J., Boquien, M., Boselli, A., *et al.* 2014, *A&A*, 568, A62

Harikane, Y., Ouchi, M., Shibuya, T., Kojima, T., Zhang, H., Itoh, R., Ono, Y., Higuchi, R., *et al.* 2018, *ApJ*, 859, 84

Inoue, A. K. 2011, *MNRAS*, 415, 2920

Itoh, R., Ouchi, M., Zhang, H., Inoue, A., Mawatari, K., Shibuya, T., Harikane, Y., Ono, Y., *et al.* 2018, ArXiv e-prints, arXiv:1805.05944

Maiolino, R., Carniani, S., Fontana, A., Vallini, L., Pentericci, L., Ferrara, A., Vanzella, E., Grazian, A., *et al.* 2015, *MNRAS*, 452, 54

Matthee, J., Sobral, D., Best, P., Khostvan, A., Oteo, I., Bouwens, R., & Rottgering, H. 2017, *MNRAS*, 465, 3637

Nagao, T., Murayama, T., Maiolino, R., Marconi, A., Kashikawa, N., Ajiki, M., Hattori, T., Ly, C., *et al.* 2007, *A&A*, 468, 877

Nakajima, K., Ellis, R. S., Iwata, I., Inoue, A., Kusakabe, H., Ouchi, M., & Robertson, B. 2016, *ApJ*, 831, L9

Olsen, K., Greve, T. R., Narayanan, D., Thompson, R., Dave, R., Niebla Rios, L., & Stawinski, S. 2017, *ApJ*, 846, 105

Ouchi, M., Ellis, R., Ono, Y., Nakanishi, K., Kohno, K., Momose, R., Kurono, Y., Ashby, M., *et al.* 2013, *ApJ*, 778, 102

Robertson, B. E., Ellis, R. S., Furlanetto, S. R., & Dunlop, J. S. 2015, *ApJ*l, 802, L19

Schaerer, D., Boone, F., Zamojski, M., Staguhn, J., Dessauges-Zavadsky, M., Finkelstein, S., & Combes, F. 2015, *A&A*, 574, A19

Shibuya, T., Ouchi, M., Konno, A., Higuchi, R., Harikane, Y., Ono, Y., Shimasaku, K., Taniguchi, Y., *et al.* 2018, *PASJ*, 70, S14

Shivaei, I., Reddy, N. A., Siana, B., Shapley, A., Kriek, M., Mobasher, B., Freeman, W., Sanders, R., *et al.* 2017, ArXiv e-prints, arXiv:1711.00013

Trainor, R. F., Strom, A. L., Steidel, C. C., & Rudie, G. C. 2016, *ApJ*, 832, 171

Vallini, L., Gallerani, S., Ferrara, A., Pallottini, A., & Yue, B. 2015, *ApJ*, 813, 36

https://doi.org/10.1017/S1743921319002618 Published online by Cambridge University Press

Discussion

Tomo Goto: The OIII/Hα turn over seems constant across a range of redshifts. But abundance might decline at higher redshifts?

Yuichi Harikane: We do not detect any significant evolution with redshift. We may be able to improve measurements with JWST.

Hiroyuki Hirashita: For the metallicity-Lyα equivalent width relation, does dust play a role?

Yuichi Harikane: We do not think so. The spectral energy distributions of Lyα emitters show a very low dust content. The dust does not significantly affect the results.

Daniel Schaerer: Whats is the lowest metallicity you obtain?

Yuichi Harikane: 2–3% solar.

Adam Carnall: Is the metallicity-Lyα equivalent width correlation being driven by the data or is it a feature of the models you are fitting?

Yuichi Harikane: From the data, the anti-correlation comes from the turnover trend of OIII/Hα.